Int J Adv Manuf Technol (2005) 27: 242–247
DOI 10.1007/s00170-004-2178-4

ORIGINAL ARTICLE

Chao Luo · Mei Zhao · Zushi Rao

The analysis of structural-acoustic coupling of an enclosure using Green's function method

Received: 2 January 2004 / Accepted: 12 March 2004 / Published online: 26 January 2005

Abstract Currently researchers expect to control the internal noise of an enclosure by controlling the relative structural vibration. The method is called ANC (Active Noise Control). Sound pressure response and velocity response of the structure are two significant factors to evaluate the performance of the ANC. But previous researches have to depend on a three-dimensional model with regular shape. Based on the Green's function theorem this paper proposed two formulas to describe the contributions of acoustic modes and structural modes. These two formulas are the essential basis for the analysis of structural-acoustic coupling of an enclosure. From them compact matrix formulas are deduced and a numerical simulation method is presented to calculate the responses of sound pressure and velocity. The numerical simulation method is verified by comparing the numerical result with the theoretical one based on a regular model. And the application of the method in an irregular model shows this method can be used to analyze any model with arbitrary shape.

Keywords Enclosure · Green's function · Modal coupling coefficient · Numerical simulation · Structural-acoustic coupling

1 Introduction

Investigating the active control of noise (ACN) within an enclosure has been a major research subject in the last several decades. Around the subject various control strategies and error criterions for controlling the sound transmission have been proposed to improve the performance of the ACN. Structural-acoustic coupling is an inevitable problem involved in the ACN. Lyon analyzed the problem of sound transmission through a panel into a rectangular cavity [1]. Dowell and Voss investigated the modal response of a cavity-backed plate [2]. Since then, there have been continuous efforts to improve the understanding of sound transmission through panels into cavities [1–13]. The previous research were based on a regular model (a rectangular enclosure with a flexible boundary). The system response can be easily gained because analytical descriptions of natural frequencies and the related modes exist if the model is regular. However, these investigations will meet difficulties if the shape of the model is irregular. In order to solve this problem, an analysis method using Green's function theory is proposed in this paper. The sound pressure response and velocity response equations are first derived theoretically and then examined by comparing the numerical result with the theoretical one. Both of them are supported by Kim's experiment [11]. These equations have obvious physical explanations and can be used for numerical simulation without the limitation of the model's shape.

C. Luo (✉) · M. Zhao · Z. Rao
Zhen Zhen Building,
Shanghai Jiao Tong University,
Min Hang District 200240, P.R. China
E-mail: luochao2000@hotmail.com
Tel.: +86-021-54741481

2 Theories

2.1 Sound pressure response equation

Let the cavity occupy a volume V, and be surrounded by a wall surface S, of which the portion S_F is flexible, while the remainder S_R is rigid. Let the fluctuating sound source $q_{\text{vol}}(\boldsymbol{x}, t)$ harmonically excite the cavity. If the air in the cavity is at rest prior to the motion of the wall, the sound pressure $P(\boldsymbol{x})$ satisfies the inhomogeneous Helmholtz equation and associated boundary condition [12]:

$$(\nabla^2 + k^2) \times P(\boldsymbol{x}) = -j\omega\rho_0 \times q_{\text{vol}}(\boldsymbol{x}) \tag{1}$$

$$\frac{\partial P(\boldsymbol{x})}{\partial n} = \begin{cases} -j\omega\rho_0 \times u_n(\boldsymbol{x}) & \text{on } S_F \\ 0 & \text{on } S_R \end{cases} \tag{2}$$

where $q_{\text{vol}}(\boldsymbol{x})$ is the fluctuating volume flow per unit volume and it is a continuous function of position vector $\boldsymbol{x}$, ρ_0 and c_0

are the equilibrium air density and acoustic velocity within the cavity, ω is the exciting frequency, $k = \omega/c_0$ is the wavenumber and $u_n(\boldsymbol{x})$ is the normal velocity of the flexible surface (positive outward).

If only one point source is considered, the sound pressure can be described by Green's function $G(\boldsymbol{x}|\boldsymbol{y})$ satisfying the equation

$$(\nabla^2 + k^2) \times G(\boldsymbol{x}|\boldsymbol{y}) = -\delta(\boldsymbol{x} - \boldsymbol{y}) \tag{3}$$

where ∇ is the Hamilton operator, and $\delta(\boldsymbol{x} - \boldsymbol{y})$ is the three-dimensional Dirac delta function.

From Eqs. 1 and 3

$$p(\boldsymbol{x}) = \int_V j\omega\rho_0 \times q_{\text{vol}}(\boldsymbol{y}) \times G(\boldsymbol{x}|\boldsymbol{y})\,\mathrm{d}V + \int_S \left[\frac{\partial p(\boldsymbol{y})}{\partial n} G(\boldsymbol{x}|\boldsymbol{y}) - p(\boldsymbol{y})\frac{\partial G(\boldsymbol{x}|\boldsymbol{y})}{\partial n}\right] \mathrm{d}S \tag{4}$$

where $G(\boldsymbol{x}|\boldsymbol{y})$ is constructed by the rigid-wall acoustic modes $\psi_n(\boldsymbol{x})$, $n = 0, 1, 2, \ldots$, with the following property:

$$\frac{\partial G(\boldsymbol{x}|\boldsymbol{y})}{\partial n} = 0 \text{ on } S \tag{5}$$

Using Eqs. 2 and 5, Eq. 4 becomes

$$p(\boldsymbol{x}) = \int_V j\omega\rho_0 \times q_{\text{vol}}(\boldsymbol{y}) \times G(\boldsymbol{x}|\boldsymbol{y})\,\mathrm{d}V + \int_{S_F} \frac{\partial p(\boldsymbol{y})}{\partial n} \times G(\boldsymbol{x}|\boldsymbol{y})\,\mathrm{d}S \tag{6}$$

Substituting Eq. 2 into Eq. 6, gives

$$p(\boldsymbol{x}) = j\omega\rho_0 \times \left[\int_V q_{\text{vol}}(\boldsymbol{y}) \times G(\boldsymbol{x}|\boldsymbol{y})\,\mathrm{d}V - \int_{S_F} u_n(\boldsymbol{y}) \times G(\boldsymbol{x}|\boldsymbol{y})\,\mathrm{d}S\right] \tag{7}$$

For a cavity with a rigid boundary, the Green's function of sound pressure can be expressed as

$$G(\boldsymbol{x}|\boldsymbol{y}) = \sum_n \frac{\psi_n(\boldsymbol{x}) \times \psi_n(\boldsymbol{y})}{\Lambda_n\left(k_n^2 - k^2 + 2j\xi_n k_n k\right)} \tag{8}$$

where $k_n = \omega_n/c_0$, ω_n and ξ_n are the natural frequency and damping ratio of the nth acoustical mode $\psi_n(\cdot)$, $\Lambda_n = \int_V \psi_n^2(\boldsymbol{x})\,\mathrm{d}V$.

Substituting Eq. 8 into Eq. 7, gives

$$p(\boldsymbol{x}) = \sum_n a_n(\omega) \times \psi_n(\boldsymbol{x}) \tag{9}$$

where

$$a_n(\omega) = \frac{\rho_0 c_0^2 \times j\omega}{\Lambda_n(\omega_n^2 - \omega^2 + 2j\xi_n\omega_n\omega)} \times \left[\int_V q_{\text{vol}}(\boldsymbol{y}) \times \psi_n(\boldsymbol{y})\,\mathrm{d}V - \int_{S_F} u_n(\boldsymbol{y}) \times \psi_n(\boldsymbol{y})\,\mathrm{d}S\right] \tag{10}$$

In Eq. 9, the acoustic pressure $p(\boldsymbol{x})$ at any location $\boldsymbol{x}$ within the cavity is expressed as an infinite summation of the product of the rigid-wall acoustic mode $\psi_n(\boldsymbol{x})$ and its related complex amplitude $a_n(\omega)$. Equation 10 indicates that the nth acoustical mode contribution $a_n(\omega)$ is from the effect of exciting sources $q_{\text{vol}}(\boldsymbol{y})$ and $u_n(\boldsymbol{y})$ on its related acoustical mode $\psi_n(\boldsymbol{y})$.

2.2 Velocity response equation

Generally, the flexible surface S_F of the cavity boundary is considered a plate or shell. Its vibration can be described by a partial differential equation

$$D \times \nabla^4(w) + \rho h\ddot{w} = p(\boldsymbol{x}, t) - \sum_l F_l(\boldsymbol{x}, t) \tag{11}$$

where ρ is the plate mass per unit area, h is the thickness of the plate, D is the bending stillness, w is the normal deflection of the plate, F_l is the lth exciting force distribution outside the flexible surface.

If harmonic excitation is considered, Eq. 11 becomes

$$D \times \nabla^4[w(\boldsymbol{x})] - \rho h\omega^2 w(\boldsymbol{x}) = p(\boldsymbol{x}) - \sum_l F_l(\boldsymbol{x}) \tag{12}$$

where $w(\boldsymbol{x})$, $p(\boldsymbol{x})$ and $F_l(\boldsymbol{x})$ are the distributions of normal deflection, sound pressure on the flexible surface and external loading, respectively.

Under a point force excitation, the normal deflection distribution of the flexible plate can be described by Green's function satisfying the equation

$$D \times \nabla^4[G(\boldsymbol{x}, \boldsymbol{x}_0)] - \rho h\omega^2 G(\boldsymbol{x}, \boldsymbol{x}_0) = \delta(\boldsymbol{x} - \boldsymbol{x}_0) \tag{13}$$

where $\delta(\boldsymbol{x} - \boldsymbol{x}_0)$ is the two-dimensional Dirac delta function.

Using the sifting property of Dirac delta function along with Eqs. 12 and 13, gives

$$D \times \int_{S_F} \left\{G(\boldsymbol{x}, \boldsymbol{x}_0) \times \nabla^4[w(\boldsymbol{x})] - w(\boldsymbol{x}) \times \nabla^4 G(\boldsymbol{x}, \boldsymbol{x}_0)\right\} \mathrm{d}S = \int_{S_F} \left[p(\boldsymbol{x}) - \sum_l F_l(\boldsymbol{x})\right] \times G(\boldsymbol{x}, \boldsymbol{x}_0)\,\mathrm{d}S - w(\boldsymbol{x}_0) \tag{14}$$

If the boundary of the flexible plate is simply supported, combining Green's theorem and the rules of the Hamilton operator gives

$$\int_{S_F} \Big\{ G(\boldsymbol{x}, \boldsymbol{x}_0) \times \nabla^4 [w(\boldsymbol{x})] - w(\boldsymbol{x}) \times \nabla^4 G(\boldsymbol{x}, \boldsymbol{x}_0) \Big\} \, \mathrm{d}S = 0 \tag{15}$$

where

$$G(\boldsymbol{x}, \boldsymbol{x}_0) = \sum_m \frac{\varphi_m(\boldsymbol{x}) \varphi_m(\boldsymbol{x}_0)}{M_m(\omega_m^2 - \omega^2 + 2j\zeta_m \omega_m \omega)} \tag{16}$$

$M_m = \int_{S_F} \varphi_m^2(\boldsymbol{x}) \, \mathrm{d}S$, $\varphi_m(\cdot)$ is the mth natural mode of the simply-supported flexible plate and ζ_m is its related damping ratio.

Substituting Eqs. 15 and 16 into Eq. 14, gives

$$w(\boldsymbol{x}_0) = \sum_m B_m(\omega) \times \varphi_m(\boldsymbol{x}_0) \tag{17}$$

where

$$B_m(\omega) = \frac{1}{M_m(\omega_m^2 - \omega^2 + 2j\zeta_m \omega_m \omega)} \times \left[\int_{S_F} p(\boldsymbol{x}) \times \varphi_m(\boldsymbol{x}) \, \mathrm{d}S - \int_{S_F} \sum_l F_l(\boldsymbol{x}) \times \varphi_m(\boldsymbol{x}) \, \mathrm{d}S \right] \tag{18}$$

Under harmonic excitation, the relation between the normal deflection $w(\boldsymbol{x}_0)$ and normal velocity $u_n(\boldsymbol{x}_0)$ of the flexible plate can be described as

$$u_n(\boldsymbol{x}_0) = j\omega \times w(\boldsymbol{x}_0) \tag{19}$$

Substituting Eq. 17 into Eq. 19, gives

$$u_n(\boldsymbol{x}_0) = \sum_m b_m(\omega) \times \varphi_m(\boldsymbol{x}_0) \tag{20}$$

where

$$b_m(\omega) = \frac{j\omega}{M_m(\omega_m^2 - \omega^2 + 2j\zeta_m \omega_m \omega)} \times \left[\int_{S_F} p(\boldsymbol{x}) \times \varphi_m(\boldsymbol{x}) \, \mathrm{d}S - \int_{S_F} \sum_l F_l(\boldsymbol{x}) \times \varphi_m(\boldsymbol{x}) \, \mathrm{d}S \right] \tag{21}$$

In Eq. 20, the normal velocity distribution of the flexible plate is expressed as an infinite summation of the product of plate mode $\varphi_m(\boldsymbol{x}_0)$ and its related complex amplitude$b_m(\omega)$. Equation 21 indicates that the mth plate mode contribution $b_m(\omega)$ is from the effect of exciting sources $p(\boldsymbol{x})$ and $\sum_l F_l(\boldsymbol{x})$ on its related plate mode $\varphi_m(\boldsymbol{x})$.

3 Numerical simulation

3.1 Matrix formulation

In order to get compact matrix formulations, rewrite Eq. 9 and Eq. 20 as Eqs. 22 and 23

$$p(\boldsymbol{x}) = \sum_n a_n(\omega) \times \psi_n(\boldsymbol{x}) \tag{22}$$

$$u_n(\boldsymbol{y}) = \sum_m b_m(\omega) \times \varphi_m(\boldsymbol{y}) \tag{23}$$

Combining Eqs. 22 and 23 along with Eq. 10 and Eq. 21, gives

$$\boldsymbol{a} = \boldsymbol{D}_n(\boldsymbol{q} - \boldsymbol{C}\boldsymbol{b}) \tag{24}$$

$$\boldsymbol{b} = \boldsymbol{D}_m(\boldsymbol{C}^T \boldsymbol{a} - \boldsymbol{F}) \tag{25}$$

where $\boldsymbol{a}$ is the Nth order vector whose nth component is $a_n(\omega)$, $\boldsymbol{b}$ is the Mth order vector whose mth component is $b_m(\omega)$, $\boldsymbol{D}_n$ is the $(N \times N)$ diagonal matrix whose diagonal components are described as

$$d_1 = \frac{\rho_0 c_0^2}{\Lambda_n(5 + j\omega)} \tag{26}$$

$$d_n = \frac{\rho_0 c_0^2 \times j\omega}{\Lambda_n(\omega_n^2 - \omega^2 + 2j\xi_n \omega_n \omega)} \quad (n > 1) \tag{27}$$

where $\boldsymbol{D}_m$ is the $(M \times M)$ diagonal matrix whose mth diagonal component is d_m, $\boldsymbol{q}$ is the Nth order vector whose nth component is q_n, $\boldsymbol{C}$ is the $(N \times M)$ coupling-coefficient matrix whose n, mth element is C_{nm}, $\boldsymbol{C}^T$ is the transposed matrix of $\boldsymbol{C}$, $\boldsymbol{F}$ is the Mth order vector whose mth component F_m is called the generalized modal force.

$$d_m = \frac{j\omega}{M_m(\omega_m^2 - \omega^2 + 2j\zeta_m \omega_m \omega)} \tag{28}$$

$$q_n = \int_V q_{\mathrm{vol}}(\boldsymbol{y}) \times \psi_n(\boldsymbol{y}) \, \mathrm{d}V \tag{29}$$

$$C_{nm} = \int_{S_F} \varphi_m(\boldsymbol{y}) \times \psi_n(\boldsymbol{y}) \, \mathrm{d}S \tag{30}$$

$$F_m = \int_{S_F} \sum_l F_l(\boldsymbol{x}) \times \varphi_m(\boldsymbol{x}) \, \mathrm{d}S \tag{31}$$

Sound pressure response (SPR) and velocity response (VR) are calculated according to the following formulations:

$$\mathrm{SPR} = 20 \log_{10} \left(\frac{|p(\boldsymbol{x})|}{p_r} \right) \tag{32}$$

$$\mathrm{VR} = 20 \log_{10} \left(\frac{|u_n(\boldsymbol{y})|}{u_r} \right) \tag{33}$$

where $p_r = 20$ uPa and $u_r = 10^{-9}$ m/s are the referenced sound pressure and velocity.

3.2 Regular model

To verify the theory and numerical simulation of this paper, the same model described in [11] is chosen. The model is a rectangular enclosure with dimensions of $L_1 \times L_2 \times L_3$, where $L_1 = 1.5$ m, $L_2 = 0.3$ m, and $L_3 = 0.4$ m. The enclosure consists of five rigid walls and a simply supported flexible plate. The plate is an aluminium plate with thickness of 5 mm.

As shown in Fig. 1, a point force is exerted at position $(13 \times L_1/30, L_2/2)$ on the plate over the frequency range 0 to 400 Hz. The related material properties are listed in Table 1.

3.2.1 Numerical simulation

The rectangular enclosure is divided into two uncoupled subsystems: a simply supported plate and a rigid-wall cavity. A total of six plate modes and four acoustic modes are calculated by the finite element method (FEM) within the frequency range of interest. The related natural frequencies are listed in Tables 2 and 3.

According Eq. 31, using the results of the FEM to calculate the coupling-coefficient matrix $\hat{\boldsymbol{C}}$, gives

$$\begin{bmatrix} 1.0000 & 0.0000 & 0.3309 & -0.0000 & 0.1956 & 0.0000 \\ 0.0000 & -0.9420 & -0.0000 & 0.3727 & 0.0000 & 0.2351 \\ 0.4749 & -0.0000 & -0.8486 & -0.0000 & -0.3318 & 0.0000 \\ -0.0000 & -0.5735 & 0.0000 & -0.8104 & -0.0000 & -0.3094 \end{bmatrix}$$

From Eqs. 32 and 33, the velocity response at position $(13L_1/30, L_2/2)$ and the sound pressure response at position $(4L_1/10, L_2/2, L_3/2)$ within the frequency range of interest can be calculated. The results are shown in Fig. 2.

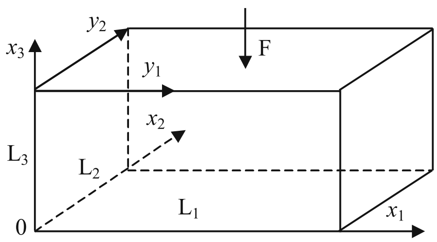

Fig. 1. Regular enclosure

Table 1. Material properties

Material	air	Al
Poisson's ratio		0.33
Modal damping ratio	0.01	0.01
Young's modulus (N/m^2)		71×10^9
Sound speed (m/s)	340	
Density (kg/m^3)	1.21	2770

Table 2. Natural frequencies of the flexible plate

Order	1	2	3	4	5	6
Frequency	140	156	183	220	268	326

Table 3. Natural frequencies of the cavity

Order	1	2	3	4
Frequency	0	113.5	227.6	343.2

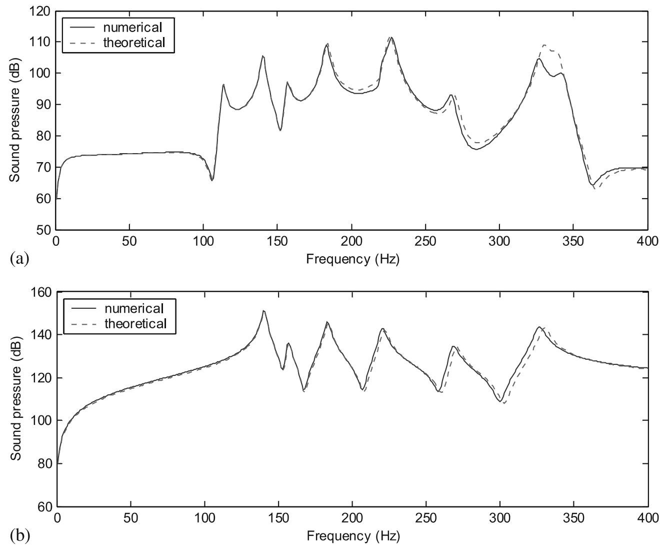

Fig. 2. a Sound responses to a point force excitation of the rectangular enclosure **b** Velocity responses to a point force excitation of the rectangular enclosure

3.2.2 Theoretical analysis

For the simply supported flexible plate of the rectangular enclosure with dimensions of $L_1 \times L_2$, its natural frequencies and the related plate modes are given by

$$\omega_m = \sqrt{\frac{D}{\rho h}} \cdot \left[\left(\frac{m_1 \pi}{L_1} \right)^2 + \left(\frac{m_2 \pi}{L_2} \right)^2 \right] \tag{34}$$

$$\varphi_m(\boldsymbol{y}) = 2 \sin\left(\frac{m_1 \pi y_1}{L_1} \right) \sin\left(\frac{m_2 \pi y_2}{L_2} \right) \tag{35}$$

where m_1 and m_2 are integers, y_1 and y_2 are the coordinate directions as Fig. 1 shows. ρ and h are the density and thickness of the aluminium plate, respectively, $D = Eh^3/[12(1-\upsilon^2)]$ is the bending stiffness, E is Young's modulus and υ is Poisson's ratio of the plate.

For the rigid-wall rectangular cavity with dimensions of $L_1 \times L_2 \times L_3$, its natural frequencies and the related acoustic modes are given by

$$\omega_n = \pi c_0 \sqrt{\left(\frac{n_1}{L_1}\right)^2 + \left(\frac{n_2}{L_2}\right)^2 + \left(\frac{n_3}{L_3}\right)^2} \tag{36}$$

$$\psi_n(\boldsymbol{x}) = \sqrt{e_1 e_2 e_3} \cos\left(\frac{n_1 \pi x_1}{L_1}\right) \times \cos\left(\frac{n_2 \pi x_2}{L_2}\right) \times \cos\left(\frac{n_3 \pi x_3}{L_3}\right) \tag{37}$$

where n_1, n_2, n_3 are integers, x_1, x_2, and x_3 are coordinate directions, $e_i = 1$ if $n_i = 0$ and $e_i = 2$ if $n_i > 0$, where subscript $i = 1,2,3$.

From Eqs. 34 and 36, the natural frequencies of the simply supported plate and the rigid-wall cavity are calculated and listed in Tables 4 and 5.

Substituting Eqs. 35 and 37 into Eq. 30, gives the coupling-coefficient matrix $\boldsymbol{C}$

$$\begin{bmatrix} 1.0000 & 0.0000 & 0.3333 & 0.0000 & 0.2000 & 0.0000 \\ 0.0000 & 0.9428 & 0.0000 & 0.3771 & 0.0000 & 0.2424 \\ -0.4714 & 0.0000 & 0.8485 & 0.0000 & 0.3367 & 0.0000 \\ 0.0000 & -0.5657 & 0.0000 & 0.8081 & 0.0000 & 0.3143 \end{bmatrix}$$

Similarly velocity response at position $(13L_1/30,\ L_2/2)$ and sound pressure response at position $(4L_1/10,\ L_2/2,\ L_3/2)$ can be gained according to Eqs. 33 and 34. The results are shown in Fig. 2.

Figure 2 shows that the sound pressure and velocity responses of the numerical simulation coincide very well with those of the theoretical analysis. Also, these results are in good agreement with the results of Kim's experiment [11].

3.3 Irregular model

What Fig. 3 shows is an irregular enclosure with dimensions of $L_a \times L_b \times h \times w$, where $L_a = 0.6$ m, $L_b = 0.75$ m, $h = 0.5$ m and $w = 0.45$ m. The enclosure consists of five rigid walls and a simply supported flexible plate. The plate is an aluminium plate with thickness of 5 mm.

Table 4. Natural frequencies of the flexible plate

Order	1	2	3	4	5	6
Frequency	141	157	184	222	270	330

Table 5. Natural frequencies of the cavity

Order	1	2	3	4
Frequency	0	113	227	340

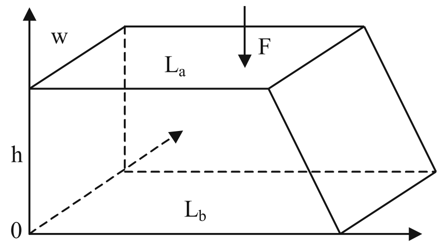

Fig. 3. Irregular enclosure

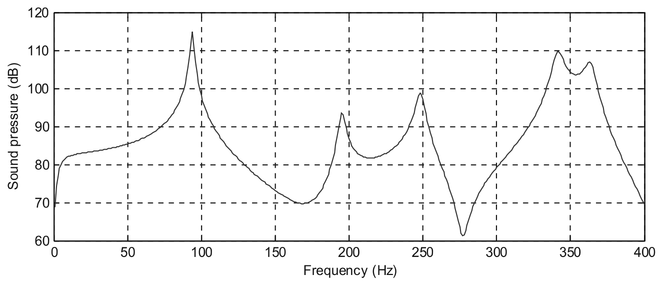

Fig. 4. Sound pressure responses to a point force excitation of the irregular enclosure

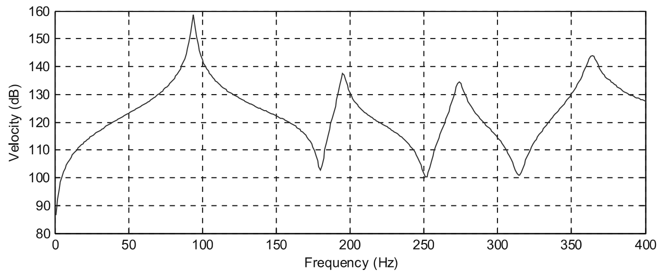

Fig. 5. Velocity responses to a point force excitation of the irregular enclosure

As shown in Fig. 3, a point force is exerted at position $(13 \times L_a/30,\ 17 \times w/30)$ on the plate over the frequency range 0 to 400 Hz. The related material properties are listed in Table 1.

The natural frequencies and the related acoustic modes of the irregular model cannot be described by analytical formulations. This is the essential difference between a regular and an irregular model. So between the numerical and theoretical methods, only the former can be used to analyse the model. Similar to the way described in Sect. 3.2.1, the velocity response at position $(13L_a/30,\ 17w/30)$ and sound pressure response at position $(2L_a/5,\ w/2,\ h)$ within the frequency range of interest can be calculated. The results are shown in Figs. 3 and 4.

4 Conclusions

Based on Green's function method, this paper proposed a set of equations to describe the modal contributions of the plate and cavity and calculate sound pressure and velocity responses.

These equations have clear physical explanations and can be easily transformed into compact matrix formulations.

Comparisons of theoretical and numerical analysis show a good agreement and they are both supported by Kim's experiment.

The example of analyzing an irregular model shows that the formulations are convenient for numerical simulation and can be used for an enclosure with any geometrical shape.

References

1. Lyon RH (1963) Noise reduction of rectangular enclosures with one flexible wall. J Acoust Soc Am 35:1791
2. Dowell EH, Voss HM (1963) The effect of a cavity on panel vibrations. Am Inst Aeronaut Astronaut J 1:476
3. Bullmore AJ, Nelson PA, Curtis ARD, Elliott SJ (1987) The active minimization of harmonic enclosed sound field, part II: computer simulation. J Sound Vib 117:15
4. Pan J (1988): A study of the active control of sound transmission through a panel into a cavity. J Acoust Soc Am Suppl 1(84):182
5. Bhattacharya MC, M.J. Crocker MJ (1969): Forced vibration of a panel and radiation of sound into a room. Acustica 22:275
6. Guy RA, Bhattacharya MC (1973) The transmission of sound through a cavity backed finite plate. J Sound Vib 27:207
7. Pan J, Hansen CH, Bies DA (1990) Active control of noise transmission through a panel into a cavity: I. Analytical study. J Acoust Soc Am 87:2098
8. Pan J, Hansen CH (1991) Active control of noise transmission through a panel into a cavity: II. Experimental study. J Acoust Soc Am 90:1488
9. Qiu XJ, Sha JZ, Yang J (1995) Mechanisms of active control of noise transmission through a panel into a cavity using a point force actuator on the panel. J Sound Vib 182:167
10. Cazzolato BS, Hansen CH (1998) Active control of sound transmission using structural error sensing. J Acoust Soc Am 104:2878
11. Kim SM, Brennan MJ (1999) A compact matrix formulation using the impedance and mobility approach for the analysis of structural-acoustic system. J Sound Vib 223:97
12. Dowell EH, Gorman GF (1977) Acoustoelasticity: general theory, acoustic modes and forced response to sinusoidal excitation, including comparisons with experiment. J Sound Vib 52:519
13. Nelson PA, Elliott SJ (1992) Active control of sound. Academic, London